Available online at www.sciencedirect.com
SCIENCE DIRECT®

Cryogenics

ELSEVIER

Cryogenics 43 (2003) 79–90

www.elsevier.com/locate/cryogenics

Performance evaluation of the ITER Toroidal Field Model Coil Phase I Part 1: current sharing temperature measurement

R. Zanino *, L. Savoldi Richard, The TFMC Testing Group

Dipartimento di Energetica, Politecnico di Torino, 24 c. Duca degli Abruzzi, I-10129 Torino, Italy

Accepted 7 January 2003

Abstract

The International Thermonuclear Experimental Reactor Toroidal Field Model Coil, a large (2.7 m $\times$ 3.8 m $\times$ 0.8 m) superconducting (Nb_3Sn) DC coil designed and constructed in collaboration between EU industries and laboratories coordinated by European Fusion Development Agreement, has been tested during 2001 in the TOSKA cryogenic facility at Forschungszentrum Karlsruhe, Germany, achieving the nominal 80 kA at 7.8 T peak field and 86 MJ stored energy as a standalone coil (Phase I). Possibly the highlight of the tests was the measurement of the current sharing temperature (T_{CS}) at different transport currents I in the self-field of the coil. The measurement method is discussed, based also on the two-year long predictive work, which preceded it. The results of the full set of T_{CS} measurements at $I = 80$, 69 and 57 kA are presented here, and evaluated in a companion paper (part 2).

Keywords: Cable in conduit conductors; Superconductors; Supercritical helium; Current sharing; Fusion magnets

1. Introduction

The Toroidal Field Model Coil (TFMC) is part of the L2 large task activities [1], which are taking place in the frame of the International Thermonuclear Experimental Reactor (ITER). The TFMC is a Nb_3Sn DC superconducting racetrack coil, pancake-wound on radial plates, and cooled by supercritical helium nominally at 4.5 K and 0.5 MPa (see Figs. 1 and 2). It was designed and constructed in collaboration between EU industries (the AGAN consortium) and laboratories, coordinated by the European Fusion Development Agreement (EFDA) [2], and tested in the TOSKA facility of Forschungszentrum Karlsruhe, Germany [3]. In the first phase of the tests, which took place during the summer and fall of 2001, the coil was tested in its self-field (peak value $\sim$ 7.8 T), while in a second phase, which should take place in the summer and fall of 2002, it will be tested under the additional field provided by the LCT coil (peak value $\sim$ 9.0 T).

The test program of Phase I included a number of items [4], starting from the achievement of the nominal operating current $I = 80$ kA, which was reached for the first time on July 25, 2001 [5]. Here we shall concentrate on the measurement of the current sharing temperature (T_{CS}) at different transport currents I. T_{CS} is calculated as the temperature where $I_C = I$, with the critical current I_C computed from Summers formula [6], and it is a major indicator of the performance of the coil. The several steps in the manufacturing (wind-react-transfer technique) and loading of the coil, and the additional complexity in defining reasonably averaged conductor parameters starting from strand data, do not generally justify the assumption that the performance of the conductor will be just as (good as) the performance of the strand, so that a dedicated experimental campaign is needed to assess also the possible change or degradation which may have occurred in the TFMC.

Although the critical current I_C should be measured at fixed temperature, it turns out that in the experiment it is much easier to control the current than the temperature, so that the T_{CS} tests are typically performed at fixed current I and increasing temperature. Indeed, there is at least one major similarity between the T_{CS} measurement method in the TFMC and those recently used on other coils, notably on the Central Solenoid Model Coil (CSMC) [7,8] and on its inserts—the Central Solenoid Insert Coil (CSIC), the Toroidal Field Conductor Insert

* Corresponding author. Tel.: +39-011-564-4490; fax: +39-011-564-4499.

0011-2275/03/$ - see front matter
doi:10.1016/S0011-2275(03)00018-3

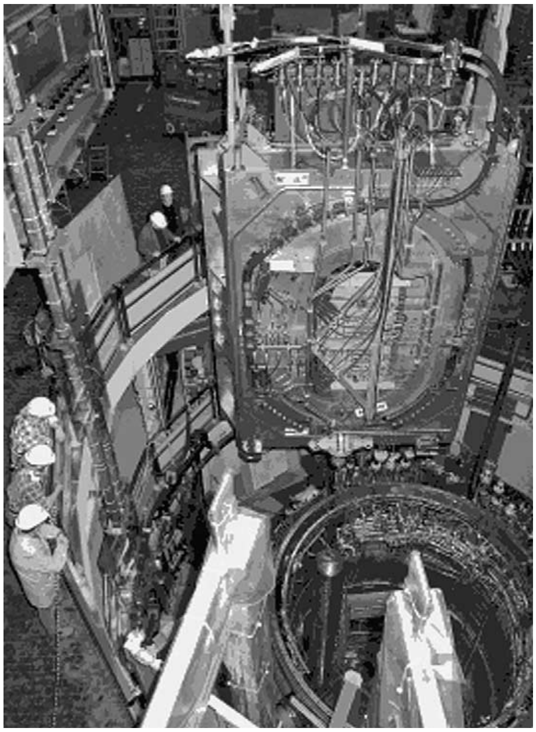

Fig. 1. The TFMC lifted over the open cryostat of the TOSKA facility at Forschungszentrum Karlsruhe, Germany, during the installation.

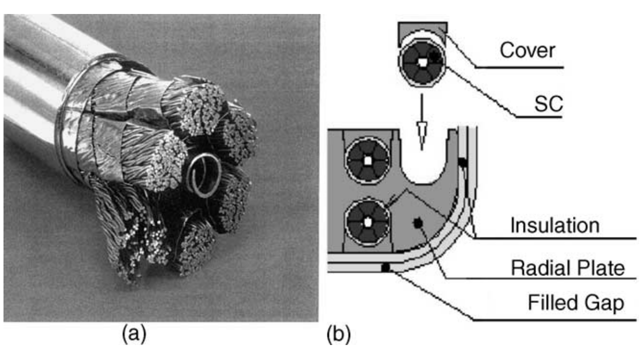

Fig. 2. (a) TFMC conductor (picture courtesy of R. Maix): inside the thin (thickness ~1.65 mm) circular 316LN jacket, 720 Nb_3Sn and 360 Cu strands are cabled in six petals around a central spiral (inner diameter ~10 mm). (b) Coil cross section: the conductor, insulated with glass/Kapton tapes, is placed inside the groove of the radial plate.

(TFCI), and the Nb_3Al Insert Coil (ALI)—all tested in 2000–2002 at JAERI Naka, Japan. In all of these coils, resistive heaters are used to increase the inlet helium temperature T_{in}, i.e., due to the large wetted perimeter, the strand temperature T_{St} inside the coil, up to T_{CS}. Some of the lessons learned from the T_{CS} tests on the CSMC, e.g., on the most suitable heating strategy, were therefore applied to the T_{CS} measurement in the TFMC (see below).

However, several peculiarities of the TFMC make the task of measuring T_{CS} particularly difficult, in comparison with what recently done on other coils. In particular:

- there are no sensors *inside* the coil (which was true also for the CSMC, while the CSIC, TFCI and ALI conductors were fairly well instrumented along their whole length), and
- the conductor length at peak magnetic field is of the order of 1 m, so that it is to be expected that the voltage measured along the coil at $I = I_C$, i.e., when the critical electric field E_C is reached (see below) will be rather low and possibly difficult to distinguish from the noise (while in the case of the CSMC the peak field region was of the order of 10 m long, thus somewhat relieving the problem).

In view of the above-mentioned peculiarities, a concerted effort of predictive analysis was set-up in 1999, i.e., well in advance of the tests. Different laboratories proposed different (heating) strategies for the T_{CS} measurements and analysed them with different computational tools. While some cursory remarks will be made on the comparison of different methods, the work done at other laboratories is mainly beyond the scope of the present paper, and we shall concentrate here on the application of the multi-step heating strategy proposed and analyzed at Politecnico di Torino using the M&M code [9,10] (see however Appendix A in the companion paper [11] for a limited M&M analysis of the only single-step T_{CS} test). The multi-step method, already used for the T_{CS} tests of the CSMC and of the CSIC, was the first to be applied to the TFMC and also the most successful in practice.

The paper is organized as follows: we describe the experimental set-up with particular reference to the T_{CS}-relevant diagnostics, and the scope of the original predictive analysis performed with M&M. Then we present the practical application of the multi-step method during the test campaign, and the results of the measurements performed at the different transport currents.

The results of the first test at 80 kA, with a somewhat different emphasis, particularly on the achievement of the original task to quench the conductor before quenching the joint (see below) were already presented in [12].

2. Experimental set-up

The TFMC is built using 5 double pancakes (DP1-5) constituted each by two ~83 m long pancakes (e.g., P2.1 and P2.2 in DP2), extreme pancakes P1.1 and P5.2 being only ~73 m long. The conductor used is the dual-channel ITER cable-in-conduit conductor (CICC), with a thin circular stainless steel (SS) jacket, and the ca-

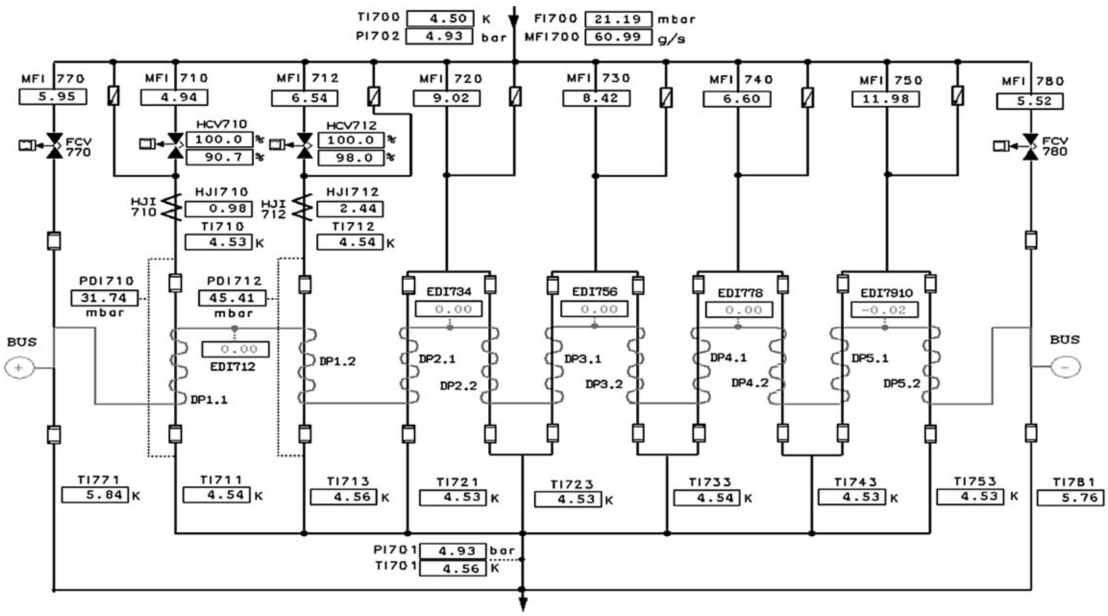

Fig. 3. Schematic view of the cryogenic circuit for the TFMC winding cooling, with approximate location of resistive heaters (HJIxxx), control valves (FCVxxx), flow meters (MFIxxx), temperature sensors (TIxxx), absolute (PIxxx) and differential (PDIxxx) pressure sensors, and joint voltage (EDIxxx) sensors, on the different pancakes DP1.1–DP5.2 and on the busbars.

ble bundle is made of 720 super-conducting strands and 360 pure Cu strands (see Fig. 2(a)). The pancakes of a given double pancake are nested on the opposite sides of SS radial plates (see Fig. 2(b)). Inner joints (with respect to the racetrack) connect the two pancakes belonging to each radial plate, while adjacent pancakes on different radial plates, e.g., P1.2 and P2.1, are connected by outer joints. The extreme pancakes P1.1 and P5.2 are jointed to the "+" and "−" NbTi busbars, respectively. All of these pancakes plus the busbars are cooled in parallel by forced circulation of supercritical helium from inner to outer joints (see Fig. 3).

The helium entering pancakes P1.1 and P1.2 may be heated independently using the resistors HJI710 and HJI712 respectively, located upstream of the conductors. These heaters are the fundamental tools for our present task of measuring the T_{CS} in the TFMC (see Fig. 3). Their location at the inlet of pancakes P1.1 and P1.2 is motivated by the fact that the peak field in the TFMC *with LCT* will be in DP1 (for the present phase without LCT the peak field is in DP3). The attempt is therefore to measure the T_{CS} on the conductor/pancake at or near peak field.

The schematic location of the most relevant sensors is given in Fig. 3: temperature measurements are available at the common inlet manifold and at the outlet of each pancake (or couple of pancakes on adjacent radial plates) and of each busbar. Pressure sensors are available at the common inlet and outlet manifolds. Mass flow rate measurements are available at the inlet of each double pancake. On the heated pancakes, additional sensors are available and namely individual measurement of the mass flow rate (MFI710, MFI712) before the heater, of the temperature (TI710, TI712) after the heater but upstream of the inlet joint, and of the pressure drop (PDI710, PDI712) along the conductor. Control valves (FCV710, FCV712) can regulate the flow in the heated pancakes. Notice again that all of the above-mentioned sensors are outside of the coil. Additionally to the thermal-hydraulic sensors, a number of sensors are available to measure the voltage drop both on the joints (EDIxxx sensors) and along whole pancakes (EKxxx and EDSxxx sensors), as discussed in detail in [12], which are also very important for our purpose.

Three different data acquisition systems (DAS) were in principle available for the T_{CS} tests in Phase I: the slow ($\sim$0.2 Hz sampling rate) cyclic DAS, the fast (from 10 to 10^4 Hz sampling rate) transient DAS, and an additional DAS named Spartan (fast data acquisition, with automatic filters resulting in an adaptive time stepping down to 5 ms, independently for each signal). However, the transient temperature data, coming from amplified raw voltage data, turned out to be significantly less accurate ($\sim\pm$0.3 K error bar) than the cyclic ones ($\sim\pm$0.01 K error bar) [13], while the cyclic temperature data could not be easily synchronized with the transient voltage data. Concerning Spartan data, they may be considered accurate only from $\sim$ mid-September on, when an additional filter was added to the measurement chain [14].

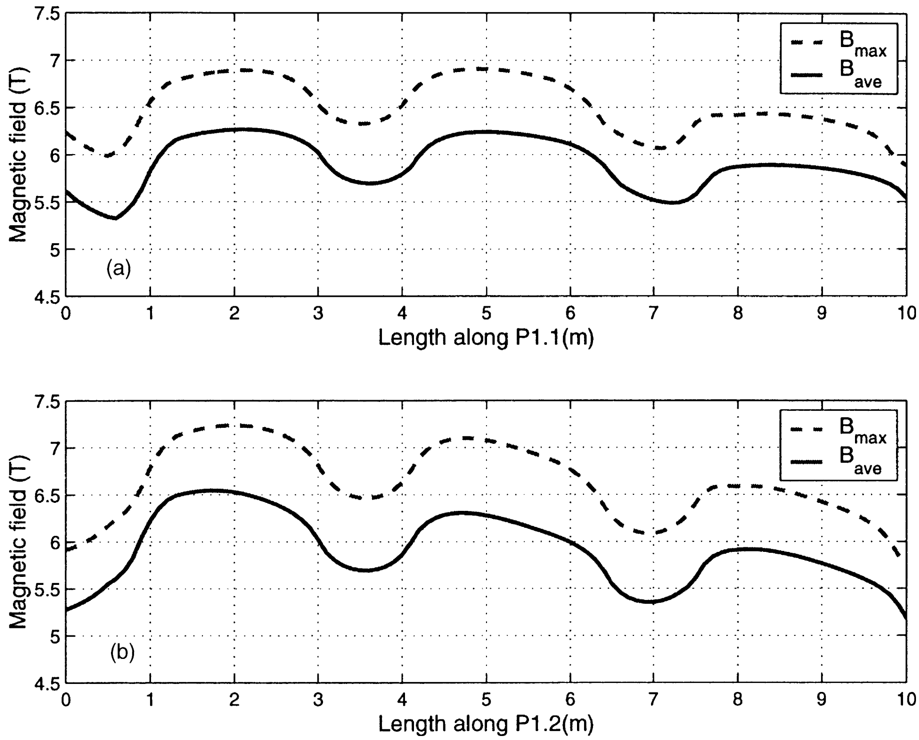

Fig. 4. Spatial profile of the maximum magnetic field (computed along the conductor inner line with respect to the coil center, dashed) and of the average magnetic field (computed along the conductor axis, solid) at 80 kA along P1.1 (a) and along P1.2 (b). Only the first 10 m of conductor are considered, including the joint. Reproduced from [15].

3. Original scope of predictive analysis with M&M and definition of the measurement method

The T_{CS} problem as it was originally posed in 1999 included two main tasks:

(1) Design a heating strategy that allows reaching the T_{CS} near peak field in the conductor [15], *without having quench propagation from the inlet joint before that happens*. This task was made particularly difficult by the fact that the properties of the joint were expected at the time to be somewhat degraded with respect to those of the conductor [16], so that even if the joint is in a somewhat lower field (see Fig. 4) the T_{CS} value there could be comparable to that in the peak field region. [1]

(2) Determine the value of T_{CS}, in the absence of sensors inside the coil. The major problem here is that one needs to relate the T_{CS}, defined in terms of *local* critical electrical field (V/m), to a *global* voltage (V) measurement, available from the experiment. Indeed it was clear from the very beginning that one should rely to some extent on codes for the assessment of the T_{CS} in the TFMC.

[1] During the experimental campaign, however, it turned out that the joints were very stable, possibly because of the large mass of copper.

By the spring of 2001, different laboratories had proposed different strategies to accomplish task 1 above [17,18]:

(a) CEA proposed and analysed with the SMART code the injection of a short (duration < 10 s) and powerful (peak > 700 W) *heat slug*; [2]
(b) CRPP proposed and analysed with the Gandalf code several *ramp* heating scenarios with different slopes and durations; [3]

[2] The heat slug strategy was never used in operation with current: the temperature and mass flow rate jumps induced by the square wave in input power, as observed in zero-current tests, turned out to be rather different compared to the expectations of previous analysis performed with the SMART code, and the whole, very transient heat slug strategy appeared to behave rather unpredictably, hardly guaranteeing that the joint would not quench before the conductor because of strongly nonlinear temperature increase at relatively high input power [19].

[3] The ramp strategy as such was never used in operation with current, as zero-current tests showed again too large overshoot in the inlet temperature T_{in}. A version modified in form of a single step, i.e., adding a short plateau to the ramp as proposed in [10], was used in a single T_{CS} test at 80 kA on September 11. Also with this single step it was possible to quench the conductor and not the joint, as desired, however the transient nature of this strategy makes the quantitative interpretation of the results in terms of T_{CS} difficult and somehow ambiguous, with significant error bars [20]. We shall present some results of the M&M analysis of this shot in Appendix A of the companion paper [11].

(c) We proposed and analysed with the M&M code several *multi-step* heating scenarios, where a series of ramp + plateau, of different slopes and durations, was used to *produce as-steady-as-possible conditions at the coil inlet*.

While it was clear from the beginning that more transient strategies as heat slug and ramps would make the analysis and interpretation of the experimental results more difficult, the main rationale behind those choices was in the limited *nominal* capacity of the TOSKA refrigeration cycle. However, it turned out later during the tests that, thanks also to the experience gained during the tests themselves, it was possible to actually operate the plant far above the conservatively foreseen nominal limits (refrigeration capacity ~1100 W and liquefaction capacity ~10 g/s for extended operation with LN_2 pre-cooling), and namely up to a refrigeration capacity of ~1700 W and to a liquefaction capacity of ~70 g/s [21].

As an interesting by-product of the predictive analysis with M&M it may also be worthwhile to observe that oscillations in the cryogenic circuit were foreseen to occur due to the operation of the heaters HJI710, HJI712 at the relatively low operating pressure ($p_{op} \sim 0.35$ MPa) originally assumed in the test program. As a consequence, p_{op} was raised to ~0.5 MPa in the tests. The predicted damping effect of increasing operating pressure was later verified experimentally (see Appendix A).

4. Implementation of the multi-step heating strategy

The multi-step strategy was implemented automatically by pre-programming a certain number of heating power steps (typically ~10–20). The same steps were applied to both HJI710 and HJI712, so that the effects of heat exchange at the common inlet joint (see Fig. 3) could be minimized, thereby also reducing the uncertainties in the interpretation of the results. A set of three parameters is sufficient to define the j-th step [12]: Q_j [W], the power at the end of the step, $\mathrm{d}Q_j/\mathrm{d}t$ [W/s], the slope of the ramp, and τ_j^{P} [s], the duration of the plateau (see also [12]). Using the critical properties from [16], including the assumption of a *total* strain of −0.5% on the conductor, and the peak B_{max} on P1.2 from Fig. 4, a *target* T_{CS} was computed at the different I, and used as reference (see below) for the design of the whole heating strategy. The design of the heating steps was such that the first few steps, thought or known to be sufficiently far from the T_{CS}, were relatively large and steep, while both the amplitude and the slope were strongly reduced in the last steps, in order to reproduce quasi-steady conditions. Besides this, an automatic ramp-down of the heaters was also eventually programmed, substituting the original manual ramp-down, and allowing to minimize the disturbance due to the heaters in the quench phase which always followed the T_{CS} test strictly speaking.

Because of a limitation of the total number of steps available in the program, the maximal programmed Q was sometimes not enough to reach the T_{CS} (see below). In these cases the progressive reduction of the mass flow rate was performed, by reducing the rpm of the circulation pump. This is already a somewhat more brutal action on the circuit than increasing the heater power by a small controlled amount, but still softer than the progressive choking of the control valves on the heated pancakes, which although available was almost never used in transient operation for that very reason.

It should also be recognized that the actual response of the circuit to the external heating was qualitatively similar but quantitatively somewhat different than observed in the predictive computations [10], also because the operating and boundary conditions (mass flow rate, pressure, etc.) were partly different. Therefore, a number of tests at zero current were needed to calibrate the effect of the heaters on the circuit; these tests led to the somehow optimised strategy, used in all of the tests at 80 kA, which is summarized in Table 1. The definition of a standard heating procedure was instrumental to guarantee some degree of reproducibility to the different tests performed at 80 kA, which were in turn relevant to verify if the performance of the coil as expressed by the

Table 1
Standard multi-step heating scenario at 80 kA[a]

Step #	Q (W)[b]	$\mathrm{d}Q/\mathrm{d}t$ (W/s)[c]	τ^{P} (s)[d]
1	218	1	150
2	240	0.5	75
3	262	0.5	75
4	271	0.5	90
5	280	0.5	140
6	289	0.5	140
7	293	0.5	140
8	297	0.5	140
9	301	0.5	140
10	305	0.5	140
11	307	0.5	140
12	309	0.5	140
13	311	0.5	140
14	313	0.5	140
15	315	0.5	140
16	317	0.5	140
17	319	0.5	140
18	321	0.5	140
19	323	0.5	140
20[e]	0	−1	–

[a] Data apply to both heaters HJI710 and HJI712, separately.
[b] Nominal final power at end of ramp (accuracy ±5%).
[c] Ramp rate.
[d] Plateau duration.
[e] Automatic ramp-down of heater power.

T_{CS} did not degrade, under the same test conditions, because of intervening quenches, as it may have happened for the CSIC [22], and for the CSMC [23,24].

As the transport current I was reduced from 80 to 69 kA, and eventually to 57 kA, the sequence of steps had to be re-determined by re-testing the effect of the heaters at zero current, using as a target the expected inlet temperature T_{in} thought to be sufficient for reaching T_{CS}. As this T_{in} is obviously a decreasing function of I, and since one needs to keep the maximum power in each heater below ~300–330 W for a safe operation of the cryo-plant, the initial mass flow rate at decreasing I was reduced in the heated pancakes, using the control valves FCV710 and FCV712.

5. Experimental results at the different transport currents (I = 80, 69, 57 kA)

In this section we present the main experimental results of the T_{CS} tests performed on the TFMC without LCT with the multi-step method.

As expected [10], in all cases the normal zone was initiated first in the P1.2 conductor, due to (nominally) equal heating in both P1.1 and P1.2, but higher mass flow rate in P1.1, and higher peak field (see Fig. 4), and therefore lower T_{CS}, in P1.2.

Although the main objective of these tests is obviously the determination of the T_{CS} itself, we do not have direct experimental evidence for this quantity on the TFMC (as seen above, the only measured temperature is the inlet helium temperature T_{in}, downstream of the heaters but upstream of the joint).

Indeed, the T_{CS} tests performed in the recent past on other ITER coils, i.e., the CSMC, the CSIC, the TFCI, or the ALI, were always based on "comparing" voltage and temperature sensor signals, making some assumptions on the extension X_N of the normal zone and, if needed, on the temperature profile along the conductor as T_{CS} was reached. Typically, for a given critical field E_C, the criterion for T_{CS} was that $T_{CS} \approx$ temperature reached at the centre of the normal zone when a voltage $\sim (E_C \times X_N)$ was measured.

However, in view of the above-mentioned TFMC peculiarities and limitations in the temperature and voltage DAS, the "usual" strategy of T_{CS} assessment cannot be used straightforwardly here, and we decide to adopt the following approach for the identification of

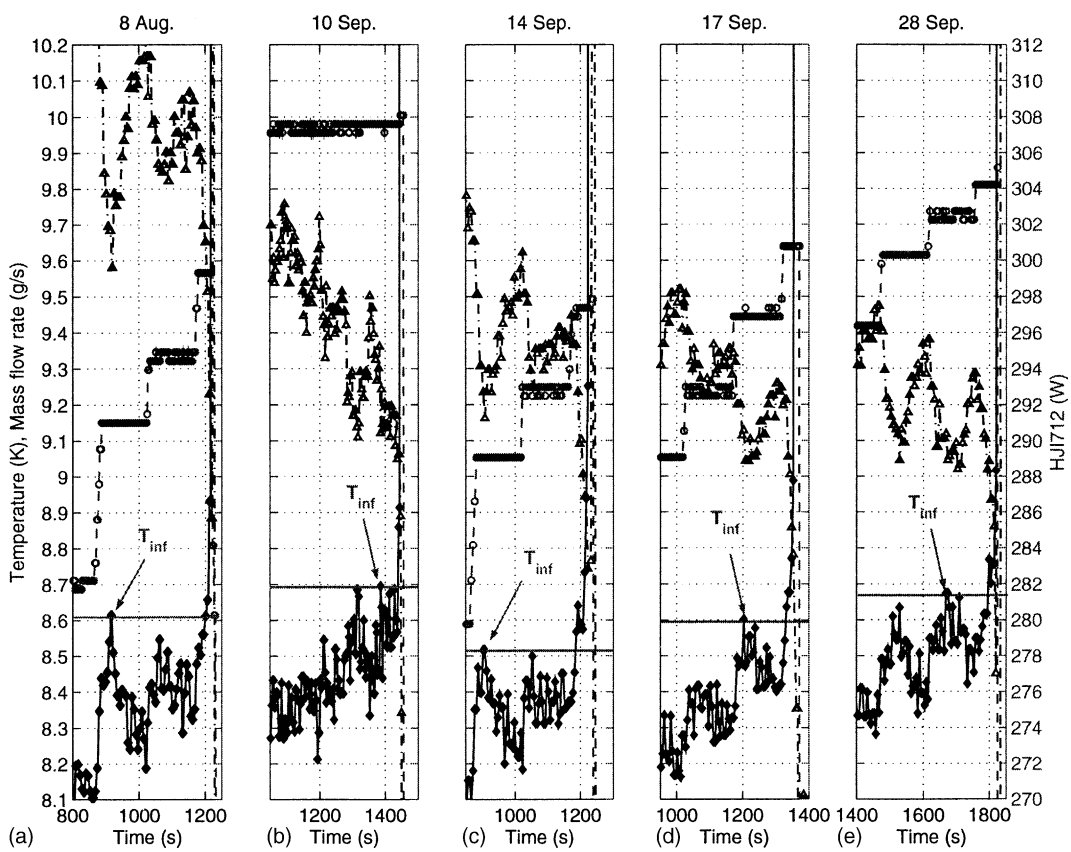

Fig. 5. Summary of the final phases of the T_{CS} measurements at 80 kA, performed in 2001 on August 8 (a), September 10 (b), September 14 (c), September 17 (d) and September 28 (e), respectively. On the left axes: evolution of the temperature TI712 (solid line, "◆" symbols) and of the mass flow rate MFI712 (dash-dotted line, triangles). On the right axis: evolution of the heating power HJI712 (dashed line, open circles). The estimated T_{inf} (see text) is also reported for each test.

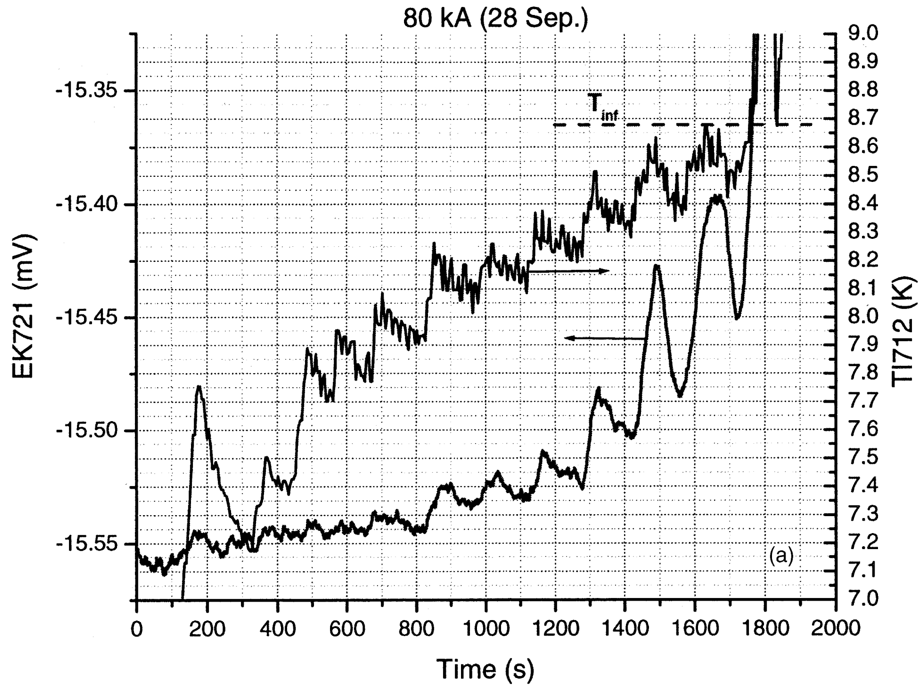

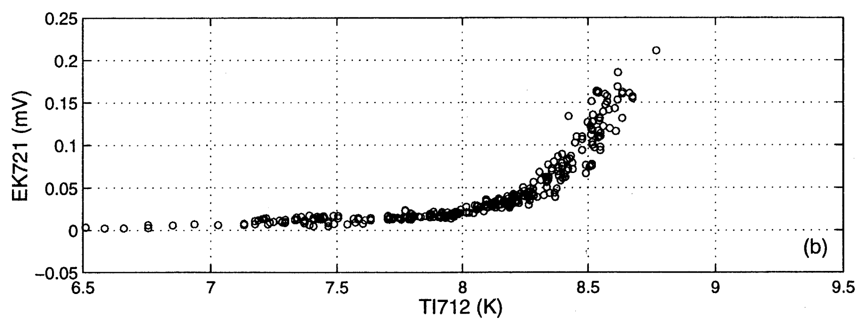

Fig. 6. T_{CS} measurement at 80 kA (September 28): (a) Evolution of the voltage drop EK721 along P1.2 measured from the Spartan DAS (right axis), and of the temperature TI712 from the cyclic DAS (right axis), synchronized by hand using as a reference the time when the heaters are switched on (not shown). The estimated T_{inf} is also reported (dashed line). (b) Corresponding voltage–temperature characteristic (baselined).

the T_{CS} starting from the experimental data collected on the TFMC:

(1) Find $T_{inf} \equiv \max(T_{in})$ not significantly influenced by Joule heating in the conductor. [4] In view of the quasi steady nature of the multi-step heating strategy, this may be considered a first zeroth order estimate of T_{CS}, based on cyclic thermal-hydraulic data only;
(2) Refine the above estimate by finding the critical parameters of the average strand in the conductor, from the M&M best fit of experimental voltage-inlet temperature characteristics (in the few cases for which they are available from the Spartan DAS, after suitable synchronization with the cyclic temperature data), and computing from Summers the corresponding T_{CS} (see [11]).

[4] We initially thought of looking for phases of the transients where, at constant external heater power and pump rpm, the mass flow rate was decreasing, which would give a clear indication of when the Joule heating downstream in the conductor started being felt. In most cases, however, it is unfortunately impossible to identify such a phase (see, e.g., Fig. 5). In practice, we shall therefore define T_{inf} as the maximum inlet temperature reached *before the last step in power* (or other control variable, e.g. pump rpm). Notice from Figs. 5, 6 that, at the T_{inf} level of voltage ($\sim$0.15 mV), the total Joule power ($\sim$12 W) is indeed still negligible with respect to the power input from the heater (>300 W). This voltage level is however already above that corresponding to the T_{CS} strictly speaking (see [11]).

5.1. Runs at $I = 80$ kA

Five T_{CS} tests were performed at 80 kA on August 8, September 10, 14, 17, 28, 2001, using the multi-step strategy. The target value of T_{CS} (as defined above) was $\sim$8.6–8.7 K. The August test ended safely with the first

TFMC full-current quench, followed by the dump (so-called safety discharge). The main thermal-hydraulic data from each of these tests are shown in Fig. 5: the evolution of conditions at the inlet of P1.2 is given as a function of time during the last heater steps before the quench occurred. It is clearly seen that each heater step leads to a temperature increase and therefore, at constant rpm, to a sudden reduction of the mass-flow rate upstream of the heater in P1.2 (and in P1.1 as well, not shown), due to its increased hydraulic resistance with respect to non-heated pancakes [10]. These jumps are followed by "recovery" phases during heater plateaus, where the mass flow rate increases again and T_{in} correspondingly decreases, except after the last step where the transient condition continues up to the quench. As mentioned above, in the singular case of September 10 (Fig. 5(b)) the maximum "acceptable" input power had already been reached without significant Joule power generation in the coil, so that the increase of T_{in} was obtained by reducing the circulation pump rpm and therefore the mass flow rate in all pancakes. (Notice that, although it would appear that on September 10 T_{in} was about the same as on August 8 (Fig. 5(a)), notwithstanding higher input power and lower mass flow rate, this apparent contradiction is due to the inaccuracy of the mass flow rate measurement itself [25]; indeed, if the pressure drop PDI712 is compared in the two cases (not shown), the larger pressure drop (i.e., mass-flow rate) corresponds to the run of September 10, as expected).

For all runs in Fig. 5 the T_{inf} estimated as discussed above is also shown, indicating that, at 80 kA, $T_{inf} \sim 8.6 \pm 0.1$ K. Indeed, one of the first nice and important consequences of the reproducibility of these runs between beginning and end of the operational campaign is that, within the tenth-of-a-Kelvin accuracy, the performance of the coil was not apparently affected by quenches.

Let us consider now as in Fig. 6(a) the evolution of the cyclic temperature data suitably synchronized (based on the common input power signals) with the measured voltage EK721 along the whole P1.2, as recorded by the Spartan system for the last quench at 80 kA. Notice first of all that the modulation in EK721 appears to be clearly correlated to the modulation of T_{in}, with increasing amplitude of the voltage oscillations, for the same amplitude of the T_{in} variations, as one approaches T_{CS}. If we interpolate now the voltage data on the less frequent temperature data we obtain the voltage-inlet temperature characteristic at 80 kA shown in Fig. 6(b), which will be used in the companion paper [11] for the interpretation of these measurements.

5.2. Run at $I = 69$ kA

In Fig. 7 we report the main experimental data of the single T_{CS} test that we did at 69 kA (corresponding to a reduction by a factor of 25% in the maximum stored magnetic energy). For this test the target value of the T_{CS} was around 9.8 K, so that, keeping the same maximum

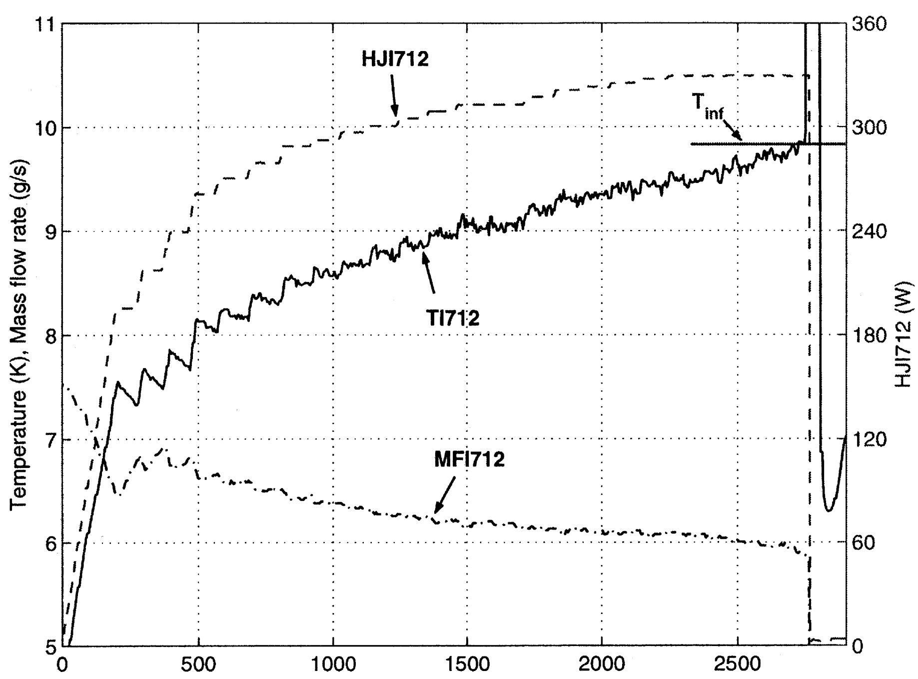

Fig. 7. T_{CS} measurement at 69 kA (September 12). On the left axis: evolution of the temperature TI712 (solid) and of the mass flow rate MFI712 (dash-dotted). On the right axis: evolution of the heating power HJI712 (dashed). The estimated T_{inf} is also reported.

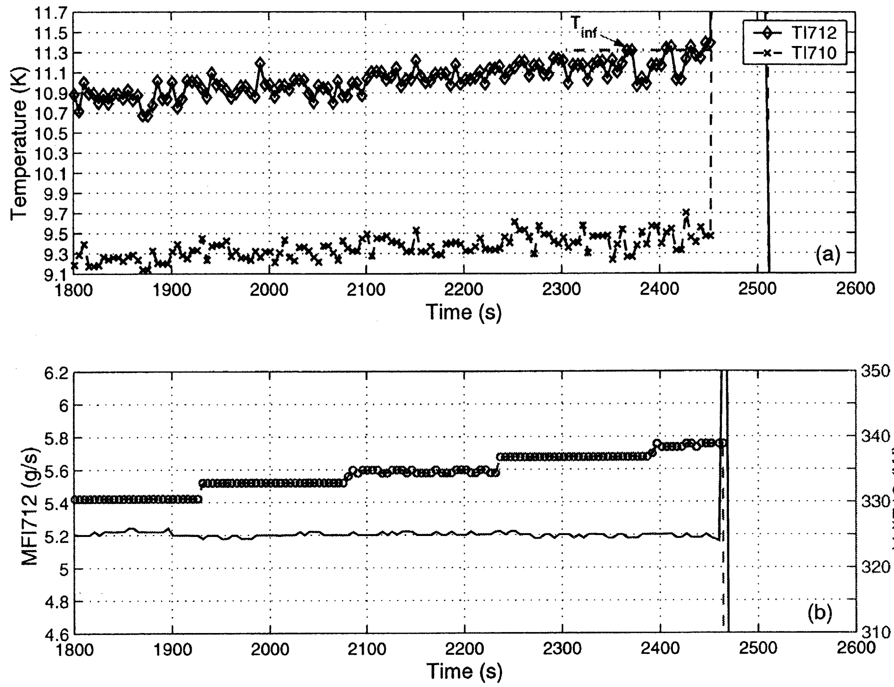

Fig. 8. Final phase of the T_{CS} measurement at 57 kA (September 13). (a) Evolution of the temperature TI712 (solid line "◇") and TI710 (dash-dotted line "×"), showing the large temperature difference between the two pancakes, which causes a strong heat exchange through the joint. The estimated T_{inf} is also reported. (b) On the left axis, evolution of the mass flow rate MFI712 (solid); on the right axis, evolution of the heating power HJI712 (dashed line "○").

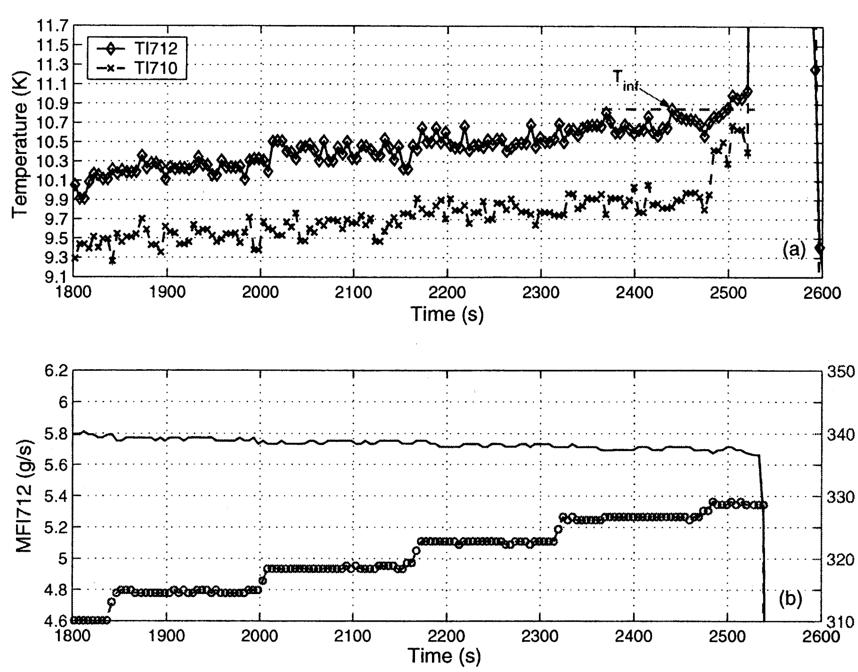

Fig. 9. Final phase of the T_{CS} measurement at 57 kA (September 27). (a) Evolution of the temperature TI712 (solid line "◇") and TI710 (dash-dotted line "×"), showing the smaller temperature difference between the two pancakes, compared to the test of September 13. The estimated T_{inf} is also reported. (b) On the left axis, evolution of the mass flow rate MFI712 (solid); on the right axis, evolution of the heating power HJI712 (dashed line "○").

heating power, a reduction of the initial mass flow rate in the heated pancakes was needed with respect to the tests at higher current. It may be noticed that, as in the September 10 run at 80 kA, the quench was initiated by reducing the mass flow rate in P1.2 at constant (maximum) heater power. In this case $T_{inf} \sim 9.8$–9.85 K but, unfortunately, no reliable V–T_{in} characteristic is available.

5.3. Runs at $I = 57$ kA

Two T_{CS} tests were performed at 57 kA, one on September 13 and one on September 27, as reported in Figs. 8 and 9 respectively. For these tests the target value of the T_{CS} was around 10.9–11 K, so that a further reduction of the initial mass flow rate in the heated pancakes was needed. On the other hand, an important and new constraint arose: since P1.1 is jointed at the outlet with the NbTi busbar, which has a limiting temperature of ~6 K [26], it was considered dangerous in the first test to raise too much the temperature in P1.1 itself, so that, with the same power input, the initial mass flow rate in P1.1 was kept higher than in P1.2 using the control valve FCV712. As a side effect, however, a relatively large temperature difference (~1.5–2 K) arose between P1.2 and P1.1, as shown in Fig. 8, which led to significant heat exchange between the two pancakes in the inlet joint, as also previously observed in dedicated tests of the Full Size Joint Sample at PSI Villigen, Switzerland [9]. The major result of this heat exchange was that $T_{inf} \sim 11.3$ K in this case, i.e., T_{in} had to rise well above the 10.9–11 K originally foreseen, before a quench could be initiated.

In order to verify if the above-mentioned speculation on the effect of heat exchange through the joint was correct, a second test was performed with a significantly increased temperature in P1.1 and therefore a significantly lower heat exchange with P1.2 in the inlet joint, which was expected to lead to a T_{in} at T_{CS} reached closer to the T_{CS} itself. Indeed, this speculation was verified in the experiment (see Fig. 9) where $T_{inf} \sim 10.8$–

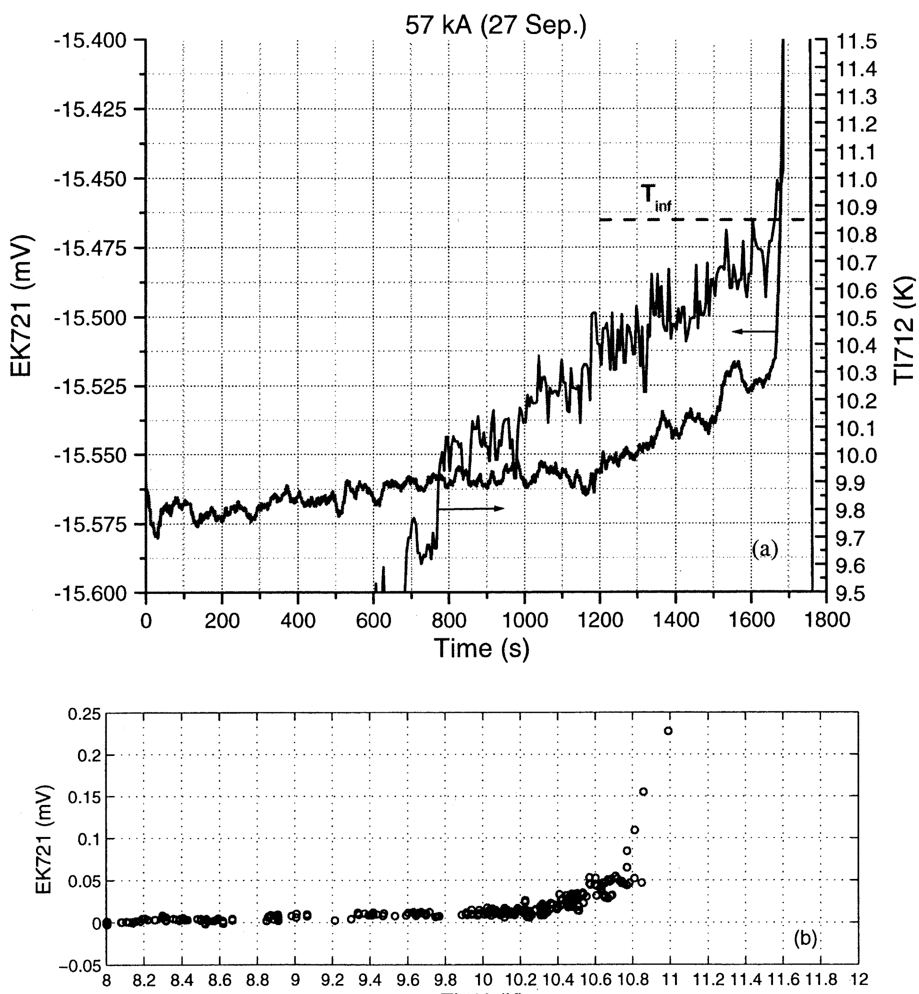

Fig. 10. T_{CS} measurement at 57 kA (September 27): (a) Evolution of the voltage drop EK721 along P1.2 measured from the Spartan DAS (right axis), and of the temperature TI712 from the cyclic DAS (right axis), synchronized by hand using as a reference the time when the heaters are switched on (not shown). The estimated T_{inf} is also reported (dashed line). (b) Corresponding voltage–temperature characteristic (baselined).

10.9 K as expected. [5] In both runs the temperature TI771 at the outlet of the busbar "+" was safely kept below 6 K.

Also for this second shot at 57 kA, reliable voltage data from the Spartan DAS are available. Therefore, we can follow the same procedure used above for the last run at 80 kA. The experimental evolution of EK721 and TI712 for this case is shown in Fig. 10(a), and the resulting V–T_{in} characteristic is shown in Fig. 10(b), to be used in the companion paper [11].

6. Conclusions and perspectives

Notwithstanding a number of difficulties peculiar of the TFMC-TOSKA, it was possible to measure the T_{CS} of pancake P1.2 successfully and sometimes repeatedly at three different transport currents, using the multi-step heating method. This was far beyond what was originally expected and planned, if one considers that the main scope of the TFMC was in a demonstration of manufacturing feasibility, in perspective of the ITER TF coils. The five tests at 80 kA showed a good reproducibility of the results within ± 0.1 K. The two tests at 57 kA showed the importance of heat exchange between P1.1 and P1.2 through the inlet joint. In two cases, measured V–T_{in} characteristics are available and are analysed in the companion paper [11] for an assessment of the TFMC performance.

The second test phase of the TFMC, this time with LCT, is planned for the summer and fall of 2002. Concerning the T_{CS} tests strictly speaking, it is planned to further apply the multi-step heating strategy as the measurement method: this will be used both for a confirmation of the results of the first phase (without LCT), and for new tests with current both in the TFMC and in the LCT. Significant improvements in the accuracy of the data should come from the planned synchronization of fast voltage and temperature measurements in the Spartan DAS.

Acknowledgements

The EFDA under the Magnetic Field Coordination of E. Salpietro partially financially supported this work as well as the position at Politecnico di Torino of LSR, whose stay at FZK was also supported by ASP and SCENET. We wish to thank the Forschungszentrum Karlsruhe, Germany, and its Superconductivity Program Leader, P. Komarek, for very kind hospitality and collaboration during the experiments.

Appendix A. Effect of increased operating pressure on reducing the oscillations in the cryogenic circuit due to external heating

One of the issues, which emerged during the long predictive work performed before the tests was that, with the originally planned value of the operating pressure $p_{op} = 0.35$ MPa at the winding outlet, temperature and mass flow rate oscillations in time appeared in the M&M simulations [10]. These oscillations, which did not appear in the simulations performed at CEA and CRPP using other computational tools, were shown *not* to be of numerical nature, and a possible physical cause for them was proposed.

These oscillations, if present and significant, could damage dramatically the quality and accuracy of the test results. Therefore, based on that qualitative explanation and on additional M&M simulations, it was suggested that if the oscillations would actually appear in the experiment, then a possible remedy could be of increasing the operating pressure to, say, 0.65 MPa.

Following this indication from the predictive analysis, the heaters HJI710 and HJI712 were never operated at 0.35 MPa, but the operating pressure was set from the beginning at $\sim$0.5 MPa. Still, it was possible to test the effect of a further increase of p_{op} to $\sim$0.6 MPa on the heater-induced oscillations in the cryogenic circuit. The result of this test, where all other control variables, and in particular the sequence of heating steps and the initial temperature and mass flow rates, were kept essentially the same, is shown in Fig. 11. It appears that the inlet temperatures in both heated pancakes indeed show somewhat reduced oscillation amplitudes by

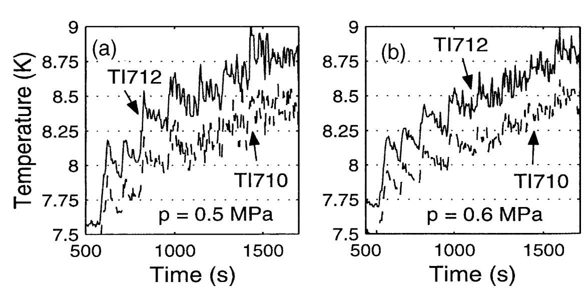

Fig. 11. Effect of the pressurization of the cryogenic circuit on the reduction of oscillations of the temperatures TI710 and TI712, downstream of the heaters HJI710 and HJI712. The same multi-step heating scenario is applied, with the only difference of an initial pressure of 0.5 MPa (a) or 0.6 MPa (b), all the other hydraulic parameters being the same.

[5] Although it would be interesting to deduce from these two tests the asymptotic value of T_{inf} corresponding to ideally zero heat exchange between P1.1 and P1.2, this is hardly possible in practice. In fact, e.g., while the temperature difference near T_{inf} is $\sim$1.6 K in the first test (Fig. 8), it is hard to identify it clearly in the case of the second test, where it drops from $\sim$1 K at T_{inf} to $\sim$0.3 K just before the quench, due to a reduction of the pump rpm.

the comparatively small increase of p_{op}, as qualitatively foreseen by the M&M simulations.

References

[1] Mizoguchi T, Mitchell N. ITER R&D: Magnets: introduction. Fusion Eng Des 2001;55:139–40;
Mitchell N, Salpietro E. ITER R&D: Magnets: Toroidal Field Model Coil. Fusion Eng Des 2001;55:171–90.

[2] Salpietro E. A toroidal field model coil for the ITER-FEAT project. IEEE Trans Appl Supercond 2002;12:623–8.

[3] Komarek P, Salpietro E. The test facility for the ITER TF Model Coil. Fusion Eng Des 1998;41:213–21.

[4] ITER Toroidal Field Model Coil test program (I): TFMC test without LCT coil, compiled by E.S. Bobrov, with contributions from Ulbricht A, Darweschsad S-M, Fink S, Heller R, Herz W, Marchese V, Wuechner F, Zahn G, Zanino R. Forschungszentrum Karlsruhe Report FE.5130.0016.0012/Z, June 2001.

[5] Fillunger H, Hurd F, Maix RK, Salpietro E, Ciazynsky D, Duchateau J-L, et al. Assembly in the test facility, acceptance and first test results of the ITER TF Model Coil. IEEE Trans Appl Supercond 2002;12:595–9.

[6] Summers LT, Guinan MW, Miller JR, Hahn PA. A model for the prediction of Nb_3Sn critical current as a function of field, temperature, strain and radiation damage. IEEE Trans Mag 1991;27:2041–4.

[7] Kato T, Tsuji H, Ando T, Takahashi Y, Nakajima H, Sugimoto M, et al. First test results for the ITER Central Solenoid Model Coil. Fusion Eng Des 2001;56–57:59–70.

[8] Savoldi L, Zanino R. Analysis of T_{CS} measurement in conductor 1A of the ITER Central Solenoid Model Coil using the M&M code. Cryogenics 2000;40:593–604.

[9] Savoldi L, Zanino R. M&M: multi-conductor Mithrandir code for the simulation of thermal-hydraulic transients in superconducting magnets. Cryogenics 2000;40:179–89.

[10] Savoldi L, Zanino R. Predictive study of current sharing temperature test in the Toroidal Field Model Coil without LCT coil using the M&M code. Cryogenics 2000;40:539–48.

[11] Zanino R, Savoldi Richard L. Performance evaluation of the ITER Toroidal Field Model Coil Phase I. Part 2: M&M analysis and interpretation. Cryogenics, this issue. doi:10.1016/S0011-2275(03)00018-3.

[12] Savoldi L, Zanino R, Marchese V, Martovetsky N, Suesser M, Ulbricht A, et al. First measurement of the current sharing temperature at 80 kA in the ITER Toroidal Field Model Coil (TFMC). IEEE Trans Appl Supercond 2002;12:635–8.

[13] Wuechner F. Operation experience: quench detection, signal conditioning, presented at the 3-rd TFMC Test Group Meeting, Forschungszentrum Karlsruhe, Germany, 22–23 January 2002. Available from: http://hikwww4.fzk.de/toska/tfmc/historyresults/3rdTFMC-TGM/talks.html.

[14] Marchese V. Private communication, 2002.

[15] Hertout P. Magnetic field calculations for the ITER Toroidal Field Model Coil, CEA Report, AIM/NTT-1999.048.

[16] Duchateau JL, Ciazynski D, Hertout P, Spadoni M, Specking W. Electromagnetic evaluation of the collective behavior of 720 twisted strands for the TF Model Coil experiment. IEEE Trans Appl Supercond 2001;11:2026–9.

[17] ITER Toroidal Field Model Coil (TFMC) test and analysis summary report Chapter 1: specific analysis results needed for testing, compiled by Libeyre P, with contributions from: Duchateau JL, Heller R, Raff S, Fink S, Hertout P, Marinucci C, Martinez A, Meyder R, Nicollet S, Savoldi L, Zahn G, Zanino R. CEA/DRFC report AIM/NTT-2001.005, May 2001.

[18] Duchateau JL, Fillunger H, Fink S, Heller R, Hertout P, Libeyre P, et al. Test program preparations of the ITER Toroidal Field Model Coil (TFMC). Fusion Eng Des 2001;58–59:147–51.

[19] Martinez A, Duchateau JL. Method for determination of the conductor current sharing temperature using travelling heat slug in the ITER TFMC. IEEE Trans Appl Supercond 2002;12: 1533–6.

[20] Marinucci C. Discussion of the T_{CS} results from the run with heater ramp, presented at the 3-rd TFMC Test Group Meeting, Forschungszentrum Karlsruhe, Germany, 22–23 January 2002. Available from: http://hikwww4.fzk.de/toska/tfmc/historyresults/3rdTFMC-TGM/talks.html.

[21] Zahn G. TOSKA operation, presented at the 3-rd TFMC Test Group Meeting, Forschungszentrum Karlsruhe, Germany, 22–23 January 2002. Available from: http://hikwww4.fzk.de/toska/tfmc/historyresults/3rdTFMC-TGM/talks.html.

[22] Martovetsky N, Michael P, Minervini J, Radovinsky A, Takayasu M, Gung CY, et al. Test of ITER Central Solenoid Model Coil and CS Insert. IEEE Trans Appl Supercond 2002;12: 600–5.

[23] Mitchell N. Assessment of the current sharing performance of layer 1A of the CSMC, April 2002, unpublished.

[24] Savoldi Richard L, Zanino R. The role of thermal-hydraulics in the ITER superconducting Central Solenoid Model Coil (CSMC) experiments. In: Proceedings of the 20-th National Conference on Heat Transfer, Maratea, Italy, 27–30 June 2002.

[25] Zanino R, Savoldi L. Considerations on thermal-hydraulic sensor accuracy", and "Pressure drop analysis in DP1 @ 4 K, presented at the 15-th TFMC Test and Analysis Meeting, 20 November 2001, CEA Cadarache, France.

[26] Maix R. Analysis of TFMC busbar behavior, presented at the 3-rd TFMC Test Group Meeting, Forschungszentrum Karlsruhe, Germany, 22–23 January 2002. Available from: http://hikwww4.fzk.de/toska/tfmc/historyresults/3rdTFMC-TGM/talks.html.